A grooved planar ion trap design for scalable quantum information processing*

Ji Wei-Bang(冀炜邦), Wan Jin-Yin(万金银), Cheng Hua-Dong(成华东), and Liu Liang(刘 亮)†

Key Laboratory for Quantum Optics and Center for Cold Atom Physics, Shanghai Institute of Optics and Fine Mechanics, Chinese Academy of Sciences, Shanghai 201800, *China*

(Received 16 September 2011; revised manuscript received 11 January 2012)

We describe a new electrode design for a grooved surface–electrode ion trap, which is fabricated in printed-circuit-board technology with segmented electrodes. This design allows a laser beam to get through the central groove to avoid optical access blocking and laser scattering from the ion trap surface. The confining potentials are modeled both analytically and numerically. We optimize the radio frequency (rf) electrodes and dc electrodes to achieve the maximum trap depth for a given ion height above the trap electrodes. We also compare our design with the reality ion chip MI I for practical considerations. Comparison results show that our design is superior to MI I. This ion trap design may form the basis for large scale quantum computers or parallel quadrupole mass spectrometers.

Keywords: ion trapping, microfabrication, quantum information

PACS: 37.10.Ty, 85.40.–e, 03.67.–a **DOI:** 10.1088/1674-1056/21/6/063701

1. Introduction

The ion trap is currently a major candidate for quantum information processing (QIP) and other quantum problems.[1−5] A practical challenge is the development of ion traps capable of storing and precisely manipulating a substantial number of ions.[6] Many typical ion traps have demonstrated QIP operations and shuttling of ions. For instance, some two-layer ion traps and three-layer ion traps have been designed for QIP. However, the complex structures of these ion traps are difficult to fabricate for scalable QIP in a large region. The surface–electrode or planar designs[7,8] with arbitrary electrode arrangements can be easily fabricated and more easily integrated with on-chip control electronics and optics.[9]

Chiaverini *et al.*[7] have proposed a planar ion trap geometry which is easy to scale up to many-zone traps and amenable to modern microfabrication techniques. All the electrodes lie in a plane and ions are trapped above the plane of the electrodes.[10] For the five-electrode planar trap design,[7] the center and outermost electrodes are held at radio frequency (rf) ground while the remaining two electrodes are biased with an rf potential for radial confinement. Either the center electrode or the outermost two electrodes can be segmented and dc biased for axial confinement. In a planar ion chip, the laser access cannot be blocked and laser scattering from ion trap surface should be avoided. The trapped ions must leave the surface of chip by some distance, which limits the ion chip's further miniaturization. One of the methods used is to cut a groove between the rf electrodes. Thus the cooling or manipulating laser beams can get through the groove. For instance, the planar ion trap geometry is designed as a Sandia trap.[11] But the Sandia trap has a complicated structure, which is fabricated using an established semiconductor integrated circuit and micro-electro-mechanical-system (MEMS) microfabrication processes. The MEMS microfabrication processes have long turn-around times and high costs. In this paper, we design a gold-on-silica planar trap geometry that is suitable for microfabrication. The ion trap design has a similar trap geometry to Chiaverini's "five wire" design with a center groove, which is used to let laser beams through. The segmented planar ion trap is fabricated by using printed-circuit-board (PCB) technology. The advantages of PCB-traps are a fast and reliable fabrication and consequently a quick turn-around time, combined with low fabrication costs.[12]

This paper is organized as follows: Section 2 pro-

*Project supported by the National Natural Science Foundation of China (Grant No. 1097421).

†Corresponding author. E-mail: liang.liu@siom.ac.cn

© 2012 Chinese Physical Society and IOP Publishing Ltd

vides an explanation of the basic concept and geometry of the trap. We also discuss how to design and optimize the size of the groove and the rf electrodes for the ion chip this section. The design of dc electrodes is also outlined in Section 2. Fabrication considerations are represented in Section 3. The practical consideration is described in Section 4. We compare the grooved planar ion trap design to a real MI I ion chip in this section. The conclusion is given in Section 5.

2. Trap design

2.1. Trap geometry

We selected a linear trap geometry with electrodes symmetrical about the trap's axial z direction. This geometry is uncommon as the symmetry causes the radial principal axes to lie in the x and y directions (see Fig. 1(a)). The trap has one pair of rf electrodes to provide the radial confinement, and 11 pairs of outer dc control electrodes for axial confinement. At present we control only the central five pairs, grounding the others. The opposite dc electrodes have the same dc voltages. We used the outer four endcap electrodes to place a static potential over the symmetric rf pseudopotential. We also show the details of the center region of the ion chip (see Fig. 1(b)). If the Doppler cooling lasers were to pass across the trap's surface, the scattering laser beams from the ion trap surface would heat the cooled ions. We chose instead to groove the central rf ground electrode (between the rf electrodes) to create a quasi "five-wire" geometry (see Fig. 1(c)). This approach causes ions to be trapped at a lower height. It meant that we could use smaller electrodes and lower rf voltage, leading to less capacitive coupling and lower losses in the rf trap drive; especially important when using a high-loss semiconductor substrate.[13] Symmetrical rf electrodes also simplify the selection of dc control voltages in complicated arrangements, such as junctions.[14] Finally, the central groove between the two rf electrodes directly below the ion can provide optical access to the ion. The design with a central groove would also simplify the laser access because some laser beams can move vertically across the groove to illuminate trapped ions. The laser scattering from the surface of electrodes can also be reduced. The symmetric trap depth of our design is as deep as the optimal "five-wire" geometry.[15] The gaps between electrodes in the trapping region are 5 μm as these can be reliably fabricated and should give a breakdown voltage of at least 400 V.[7] Small gaps between the trap electrodes in realistic geometries often have negligible effects on trap parameters.[16]

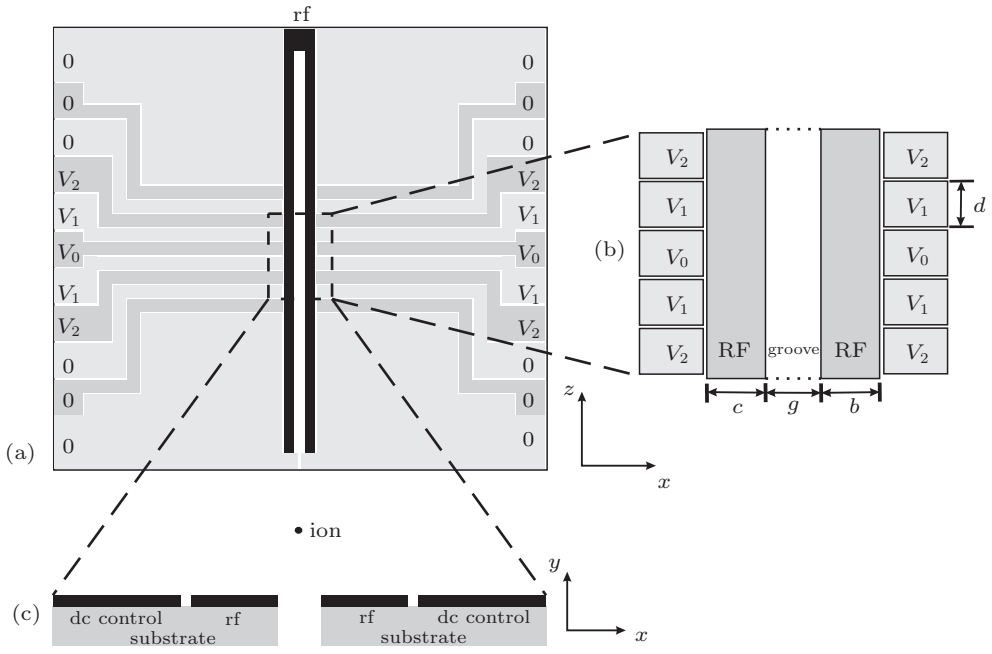


Fig. 1. Trap design: (a) plan view. The rf rails are dark grey and the dc control electrodes are alternately picked out in light/medium grey for clarity. The labels refer to the different voltages, V_0, V_1, V_2, we apply. Other dc electrodes are grounded (0). (b) Details of the trapping region. This design with outer segmented static electrodes and rf electrodes separated by a center groove. (c) End view showing electrodes, gaps, and ion position.

2.2. The rf electrode design and optimum

The dynamics of an ion in a linear rf Paul trap are determined by solving the classical equations of motion.[17] For an rf quadrupole ion trap, the electric potential can be presented as

$$\phi(x,y,t)=\frac{x^2-y^2}{2{r_0}^2}(U-V\cos\Omega t), \tag{1}$$

where r_0 is the distance between ion and electrodes, U is the DC voltage applied to the dc electrodes and V is the AC voltage amplitude applied to the rf electrodes, Ω is the rf drive frequency. The x and y equations of motion can be transformed into the form of Mathieu equations

$$\frac{\mathrm{d}^2x}{\mathrm{d}\tau^2}+[a-2q\cos(2\tau)]x=0, \tag{2}$$

$$\frac{\mathrm{d}^2y}{\mathrm{d}\tau^2}+[a-2q\cos(2\tau)]y=0. \tag{3}$$

Here $\tau=\Omega t/2$ is a dimensionless time, the Mathieu parameters $q=2QV/mr_0^2\Omega^2$ and $a=4QV/mr_0^2\Omega^2$ are dimensionless rf and dc voltages, Q and m are the ion charge and mass. The stable region of ion motion is $0<q<q_{\max}=0.908$ for $a=0$ in a–q parameter regions.

In the pseudopotential approximation, where $q\ll 1$, the ion motion along axis i ($i=x,y,z$) can be decomposed into two parts: one is slow, large amplitude secular motion at the secular frequency $\omega_i=QVf_i/\sqrt{2}mr_0^2\Omega$; the other is fast, small amplitude micromotion at the rf drive frequency Ω. Neglecting the micromotion: a reasonable approximation for $|q|\ll 1$, we can define an approximate harmonic potential that describes the ion motion near the quadrupole zero by the following equation

$$\Psi(y)=\frac{1}{2}m\omega_y^2(y-y_0)^2=\frac{Q^2V_{\mathrm{rf}}^2}{4mr_0^4\Omega^2}(y-y_0)^2, \tag{4}$$

where $\omega_y=QVf_y/\sqrt{2}mr_0^2\Omega$, especially $f_i=1$ for a perfect quadrupole trap and we consider the secular frequency in the harmonic region of the potential where it is the same along x,y,z axes.[14] The harmonic potential of Eq. (4) provides an intuitive connection to the time-averaged motion of the trapped ion in the vicinity of the rf node, but it does not reveal any information about the dynamics if the inequality $|y-y_0|\ll y_0$ is not satisfied. For instance, in a real device there is a finite trapping volume and trap depth. These quantities originating from the shape of the potential are significantly beyond the harmonic region. In the limit $|q|\ll 1$, the effective potential energy beyond the harmonic regime is commonly referred to as the ponderomotive pseudopotential. It may be expressed directly by the gradient of the electric potential as[18]

$$\Psi(x,y,z)=\frac{e^2}{4m\Omega^2}|\bigtriangledown\phi_{\mathrm{rf}}(x,y,z)|^2, \tag{5}$$

where e, m, and Ω are electric charge, mass, and rf drive frequency, respectively. ϕ_{rf} represents rf potential. In a surface ion trap, the rf electrodes produce the rf field and create a local pseudopotential minimum above the electrode surface along the y direction, where ions can be trapped as shown in Fig. 2. The pseudopotential has a saddle point above the surface center, which is the turning point for an ion trapped inside the pseudopotential well to escape from the trap. Beyond this point, the pseudopotential approaches zero when $y\to\infty$. The pseudopotential at this "escape point" represents the depth of the trap if $\Psi=0$ at the trap center.

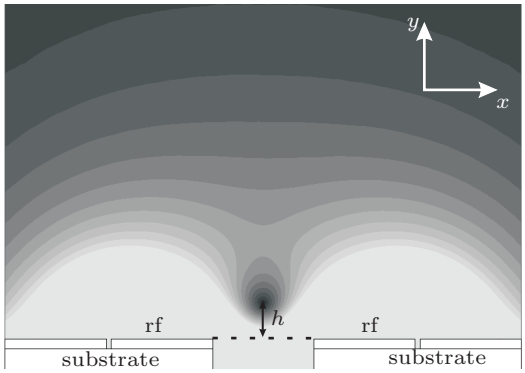


Fig. 2. Illustration of pseudopotential field over the surface trap. h is the distance between a trapped ion and surface electrodes, and the escape point for the ion is located well beyond h.

The solid line in Fig. 3 shows the effective pseudopotential along the y direction for the planar ion Paul trap. The superimposed line is the harmonic approximation (dashed line). This pseudopotential approximation is useful to characterize the trap depth of the ion trap. The location of this minimum is the trap center. According to our design, the length of the z direction can be considered as infinity. As the potential field described in Ref. [19],

$$\phi_{\mathrm{rf}}(x,y,t)=\frac{V_{\mathrm{rf}}}{\pi}\left[\arctan\left(\frac{g+b-x}{y}\right)-\arctan\left(\frac{g-x}{y}\right)-\arctan\left(\frac{x}{y}\right)\right.$$

$$+ \arctan\left(\frac{c+x}{y}\right)\Bigg]\cos(\Omega t), \qquad (6)$$

where g is the width of the groove, b and c are widths of rf electrodes, Ω is the rf drive frequency. The ion is located at $y_0 = \sqrt{gbc(g+b+c)/(b+c)}$, which is the coordinate of the pseudopotential minimum. The escape point y_E denotes the turning-point of the confining pseudopotential. It can be found by using the numerical method for the point above the trap center where the gradient of the pseudopotential is zero. The trap depth at the escape point for the ion trap can be found in Ref. [20]

$$\Psi = \frac{e^2}{4m\Omega^2h^2} \times \left[\frac{2\sqrt{gbc(g+b+c)}}{(2g+b+c)(2g+b+c+\sqrt{g(g+b+c)})}\right]^2, \qquad (7)$$

where h is the distance between the position of trapped ions and the surface electrodes. By choosing appropriate electrode widths, the trap geometries can be optimized to achieve the maximum trap depth for a given ion height. In the surface trap geometries shown in Fig. 1, two rf electrodes have the same width ($b = c$). If the ratio $\alpha = b/g$, which is the ratio between the rf electrode width b and the groove size g between rf electrodes, Eq. (7) can be described as[20]

$$\Psi = \frac{e^2V_{rf}^2}{\pi m\Omega^2h^2}\left[\frac{\alpha(1+2\alpha)}{4(1+\alpha)^2(1+\alpha+\sqrt{1+2\alpha})^2}\right]^2. \qquad (8)$$

For a given ion height, the value of $e^2V_{rf}^2/\pi m\Omega^2h^2$ is constant. We only consider the function of α, which decides the depth of the surface ion trap. The maximum of the function can be found at $\alpha \simeq 3.68$ for equal widths of rf electrodes. For the optimized value of α, the ion height above the electrodes is given by $h = 0.39b$ for the equal width rf electrodes.[20] We also calculated the distribution of the pseudopotential field by using the finite element analysis method (FEAM) with fixed widths of rf electrodes and ion height. The trap depth can be defined as $\Psi = \Psi(y_E) - \Psi(y_0)$. As the pseudopotential shown in Fig. 3, $\Psi(y_0)$ can be considered as zero, $\Psi = \Psi(y_E)$. According to Eq. (5), the trap depth $\Psi \propto |E|^2$, where $|E|$ is the electric field intensity at "escape point". Variation values of $|E|^2$ are plotted by changing the value of α, which are shown in Fig. 4. It is seen that, in accordance with the analytical model, the trap depth has the maximized value at $\alpha \simeq 3.7$. The simulated value of the optimized ion height is about 36 μm ($g = 27.2$ μm, $b = 100$ μm). The trapping potential becomes weaker if the rf electrodes are too narrow or too wide relative to the center electrode. From these calculations, we are able to extract an optimal radial trap in the absence of dc potentials. It is very useful to make a 2D ion trap array for scalable quantum information and quantum computer design.

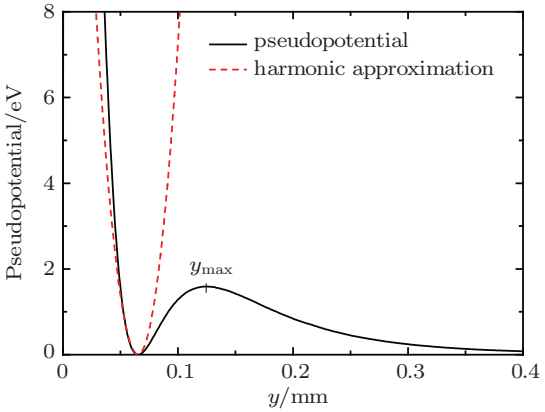


Fig. 3. (colour online) The harmonic potential approximation [from Eq. (4); dashed line] for the surface ion trap on top of the pseudopotential Eq. (5); solid line.

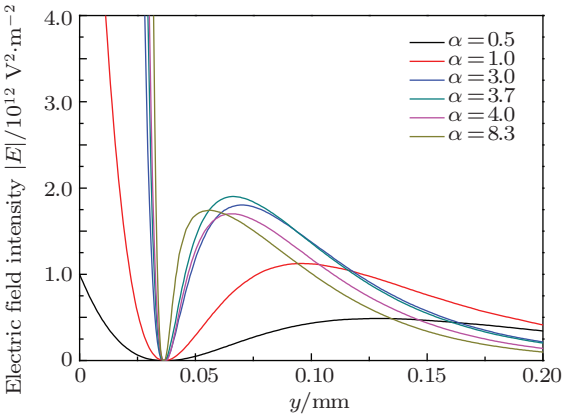


Fig. 4. (colour online) Variation of electric field intensity $|E|^2$ with equal width rf electrodes ($b = c$) at various values of α. The maximum value of $|E|^2$ at the "escape point" is obtained when the ratio between the rf width and groove is $\alpha \approx 3.7$.

2.3. The dc electrode design

Linear Paul traps are characterized by two-dimensional dynamical confinement in the radial direction (x–y plane) and static confinement in the axial direction (z axis). We have described the radial optimization of the linear Paul trap. Then the axial electrode geometry is calculated based on the optimal radial geometry. In our design, the dc electrodes can be achieved by segmenting the outer rf grounded electrodes. For axial confinement, opposing dc electrodes

are set to the same voltage V_i $(i = 0, 1, 2)$ labeling the electrode number as depicted in Fig. 1. These voltages can be supplied by D/A converters covering a voltage range of ±30 V. For arbitrary voltage configurations, the axial potential $\Phi(z) = \sum_i V_i \Phi_i(z)$ is a linear superposition of the single electrode potentials. A numerical curve illustrates the sum potentials shown in Fig. 5. It suggests that axial confinement can also be provided for our trap.

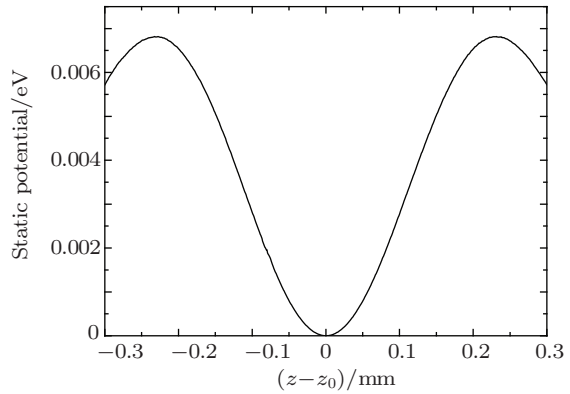


Fig. 5. The sum of static potentials varied along the z direction. It means that the ion can be trapped in z direction in our design.

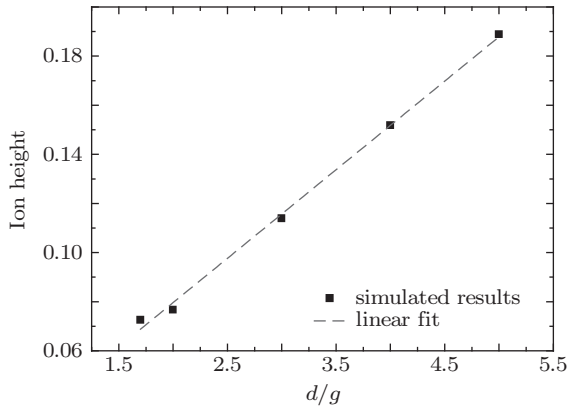


Fig. 6. The ion height (scattering points) is plotted against the ratio between dc electrodes width d and groove size g for optimum value of α. The optimized value d is obtained by using fitting curve (straight line), and it is $0.9g$.

We also provide the optimum width of dc electrodes for the ion trap design. The widths of static potential electrodes should be chosen in such a way that they provide the same ion height of the potential at the center of the trap in the z direction. For this purpose, we fix the optimum rf electrode width, as already discussed for a maximum trap depth at given ion height, being approximately $3.7g$. Assuming that all the dc electrodes have the same size d as shown in Fig. 1, we have calculated the ion height by varying the dc electrode widths. In Fig. 6, the ion height is plotted against the ratio of dc electrode d width to groove size for surface trap designs. Then we make the linear fit to this plot, and the suitable width of the static potential electrodes is about $0.9g$ for the design.

3. Fabrication considerations

There are several different processes that could be used to fabricate these micro ion traps: (i) silicon-based micro-electro-mechanical machining (MEMS) techniques; (ii) gallium–arsenide (or other suitable materials) based molecular-beam epitaxy (MBE) grown wafers and associated etching processes; (iii) other relevant techniques such as anodic wafer bonding or flip-chip technologies. However, most of these fabrication methods require advanced and non-standard techniques of micro-fabrication. Long turn-around times and high costs are making progress in ion trap development more complicated. In this paper, we present a segmented planar ion trap which is fabricated in UHV-compatible printed-circuit-board (PCB) technology. By using this technology, the spatial dimensions of the electrodes are typically limited to more than 100 μm, the production of sub-millimeter sized segments is simplified by the commonly used etching process. The advantages of PCB-traps are therefore a fast and reliable fabrication and consequently a quick turn-around time, combined with low fabrication costs.[21] The feasibility of the PCB technique for trapping ion clouds in a surface–electrode trap has already been shown in Ref. [22]. In future, we anticipate an enormous impact of PCB technology by including standard multi-layer techniques in the trap design.

The trap electrode material is considered as gold, and the substrate is SiO_2. As in the surface electrode trap, the gold electrodes in our trap design have low resistive impedance, and the SiO_2 dielectric has a low capacitive reactance. The rf losses (and subsequent heating of the trap chip) are calculated to be significantly lower than those in the GaAs trap. Thus our designed trap is expected to exhibit a deep potential well, a high trap efficiency, and a low rf loss, which are in contrast to some features of the other microfabricated traps. These differences will contribute to an increased understanding of ion trap materials and structures for QIP applications. The trap strength may be

limited by the maximum voltage that can be applied to the electrodes before the occurrence of electric field breakdown. The theoretical limit to the breakdown voltage is dependent on the bandgap of the semiconductor material and, for Si and GaAs, is on the order of 40 V/μm–50 V/μm and for silica, on the order of 80 V/μm.[7] In our design, for electrodes separation of 5 μm, the maximum applied voltage is expected to be of the order $V_0 = 400$ V.

4. Practical consideration

Beyond demonstrating that the proposed design will provide suitable trapping potentials for QIP applications, we also calculate several practical factors, which include the secular frequency, axial frequency, ion height, and trap depth. We calculate these factors with $^{111}Cd^+$ for $V_{rf} = 370$ V at $\Omega/2\pi = 32$ MHz, $V_2 = 30$ V and other electrodes at 0 V. We choose the same rf electrodes width $b = 370$ μm as in Ref. [24], then the groove size is $g = 100$ μm and widths of DC electrodes are 90 μm. The ion height is calculated as 144 μm. The calculated value of secular frequency ω_x, ω_y, and axial frequency ω_z are also obtained by using the theory in Ref. [23]. They are 6.26 MHz, 5.58 MHz, and 1.53 MHz, respectively. In order to verify the feasibility of our design, we compare our factors with a planar ion trap MI I at Michigan University.[24] This planar trap is a "quasi five wire" trap. The results are displayed in Table 1.

Table 1. Comparison between an Osaka ion chip and our design.

Parameter	MI I trap	Our design
Ion height h/μm	79	144
rf voltage V_0/V	370	370
rf trap drive	370 V at 32 MHz	370 V at 32 MHz
Trap depth/eV	0.50	0.66
End-cap voltage/V	15	30
Secular frequencies/MHz	5.7, 5.9, 0.5	4.20, 5.58, 1.53

As shown in Table 1, the ion height of our design is higher than MI I. Simultaneously, we have a larger trap depth. It suggests that trapped ions are more stable with our design. The secular motion of trapped ions is determined by secular frequencies with fixed applied voltages.[23] According to the results, we obtained smaller secular frequencies than MI I, it means trapped ions in our design have smaller secular motion than in MI I, i.e., our design is superior to the MI I. Our design has the high feasibility in our future experiments.

5. Conclusion

We have proposed a novel grooved planar ion trap design for quantum information processing. The planar symmetric trap structure, which can be microfabricated on a chip using PCB processing techniques, is of significant interest for implementations of QIP using trapped ions. The trap electrodes are formed by using gold, and are spaced by silica. The pseudopotential of the ion trap has been calculated analytically by using House's model.[19] We have also obtained the numerical solution by using the FEAM. The analytical and simulated results are coincident with each other. The optimized rf electrode structure has been described in this paper. The dc electrode design has also been calculated by using the FEAM, and it shows that ions can be trapped axially. Additionally, we have demonstrated that the planar ion trap design must consider the appropriate fabrication method. Finally, we compare our design with the reality ion chip MI I. The comparisons of our results with theirs show that our design is superior to the MI I. Planar ion traps are a general tool used in many applications in quantum simulation, quantum computation, and mass spectrometry. Using modern two-dimensional fabrication techniques, the traps described here can be reconstructed to be compatible with UHV and atomic ions. Furthermore, the gold-on-silica trap chip design is feasible. And it has the potential to form the basis of large-scale ion trap quantum processors.

References

[1] Home J P, Hanneke D, Jost J D, Amini J M, Leibfried D and Wineland D J 2009 *Science* **325** 1227

[2] Liu W Y, Bi S W and Dou X B 2009 *Acta Phys. Sin.* **59** 1780 (in Chinese)

[3] Yang M R, Hai W H, Lu G B and Zhong H H 2010 *Acta Phys. Sin.* **59** 2406 (in Chinese)

[4] Ai L Y, Yang J and Zhang Z M 2008 *Acta Phys. Sin.* **57** 5589 (in Chinese)

[5] Chen W Q, Hai W H and Song J W 2008 *Acta Phys. Sin.* **57** 1608 (in Chinese)

[6] Kielpinski D, Monroe C and Wineland D J 2002 *Nature* **417** 709

[7] Chiaverini J, Blakestad R B, Britton J, Jost J D, Langer C, Leibfried D, Ozeri R and Wineland D J 2005 *Quantum Infor. Comput.* **5** 419

[8] Stahl S, Galve F, Alonso J, Djekic S, Quint W, Valenzuela T, Verdú J, Vogel M and Werth G 2004 *Eur. Phys. J.* D **32** 139

[9] Wan J Y, Wang Y Z and Liu L 2008 *Chin. Phys.* B **17** 3565

[10] Janik G R, Prestage J D and Maleki L 1990 *J. Appl. Phys.* **67** 6050

[11] Imreh G 2008 "Implementing Segmented Ion Trap Designs for Quantum Computing" *Ph. D. Thesis* (University of Oxford)

[12] Brownnutt M, Wilpers G, Gill P, Thompson R C and Sinclair A G 2006 *New J. Phys.* **8** 232

[13] Leibrandt D R, Labaziewicz J, Clark R J, Chuang I L, Epstein R J, Ospelkaus C, Wesenberg J H, Bollinger J H, Leibfried D, Wineland D, Stick D, Stick J, Monroe C, Pai C S, Low Y, Frahm R and Slusher R E 2009 *Quantum Infor. Comput.* **9** 901

[14] Amini J M, Britton J, Leibfried D and Wineland D J 2008 *Microfabricated Chip Traps for Ions Atom Chips* (New York: Wiley)

[15] Pearson C E, Leibrandt D R, Bakr W S, Mallard W J, Brown K R and Chuang I L 2007 *Phys. Rev.* A **73** 032307

[16] Roman S 2010 *New J. Phys.* **12** 023038

[17] Ghosh P K 1995 *Ion Traps* (Oxford: Clarendon Press)

[18] Dehmelt H G 1967 *Adv. At. Mol. Phys.* **3** 53

[19] House M G 2008 *Phys. Rev.* A **78** 033402

[20] Ji W B, Wan J Y, Cheng H D and Liu L 2008 *Chin. Phys. Lett.* **28** 073701

[21] Kumakura M, Shirahata Y, Takasu Y, Takahashi Y and Yabuzaki T 2003 *Phys. Rev.* A **68** 021401

[22] Brown K R, Clark R J, Labaziewicz J, Richerme P, Leibrandt D R and Chuang I L 2007 *Phys. Rev.* A **75** 015401

[23] Berkeland D J, Miller J D, Bergquist J C, Itano W M and Wineland D J 1998 *J. Appl. Phys.* **83** 5025

[24] Leibrandt D R, Labaziewicz J, Clark R J, Chuang I L, Epstein R J, Ospelkaus C, Wesenberg J H, Bollinger J J, Leibfried D, Wineland D J, Stick D, Sterk J, Monroe C, Pai C S, Low Y, Frahm R and Slusher R E 2009 *Quantum Infor. Comput.* **9** 901